

1 Research Article

2

3 **L-Malic Acid Production from Xylose by Engineered *Saccharomyces Cerevisiae***

4

5 Nam Kyu Kang^{1,2}, Jae Won Lee^{2,3}, Donald R. Ort^{1,2,4}, Yong-Su Jin^{1,2,3}

6

7 ¹Carl R. Woese Institute for Genomic Biology, University of Illinois at Urbana -

8 Champaign, Urbana, IL, USA

9 ²DOE Center for Advanced Bioenergy and Bioproducts Innovation, University of Illinois

10 at Urbana - Champaign, Urbana, IL, USA

11 ³Department of Food Science and Human Nutrition, University of Illinois at Urbana -

12 Champaign, Urbana, IL, USA

13 ⁴Departments of Plant Biology and Crop Sciences, University of Illinois at Urbana-

14 Champaign, Urbana, Illinois, USA

15

16 **Correspondence:** Dr. Yong-Su Jin, Department of Food Science and Human Nutrition,

17 University of Illinois at Urbana - Champaign, Urbana, IL, USA.

18

19 **E-mail:** ysjin@illinois.edu

20

21 **Keywords:** C4-dicarboxylic acids, malic acid, metabolic engineering, *Saccharomyces*

22 *cerevisiae*, xylose

23

24 **Abbreviations:** **XI**, xylose isomerase; **XR**, xylose reductase; **XDH**, xylitol
25 dehydrogenase; **GRAS**, generally recognized as safe; **TCA**, tricarboxylic acid; **rTCA**,
26 reductive TCA; **PYC**, pyruvate carboxylase; **MDH**, malate dehydrogenase; **FUM**,
27 fumarase; **FRD**, fumarate reductase; **alsS**, acetolactate synthase; **alsD**, α -acetolactate
28 decarboxylase; **ADH**, alcohol dehydrogenase; **PDC**, pyruvate decarboxylase; **GPD**,
29 glyceraldehyde-3-phosphate dehydrogenase; **ME**, malic enzyme; **SpMAE1**,
30 *Schizosaccharomyces pombe* malate transporter; **OD₆₀₀**, optical density at 600 nm;
31 **HPLC**, high performance liquid chromatography; **DCW**, dry cell weight; **DHAP**,
32 dihydroxyacetone phosphate; **GAP**, glyceraldehyde-3-phosphate; **G3P**, glycerol-3-
33 phosphate; **xylulose-5-P**, xylulose-5-phosphate

34 **Abstract**

35 L-malic acid is widely used in food, chemical, and pharmaceutical industries. Here, we
36 report the production of malic acid from xylose, the second most abundant sugar in
37 lignocellulosic hydrolysates, by engineered *Saccharomyces cerevisiae*. To enable malic
38 acid production from xylose, *PYC1* and *PYC2* coding for pyruvate carboxylase, a
39 truncated *MDH3* coding for malate dehydrogenase, and *SpMAE1* coding for
40 *Schizosaccharomyces pombe* malate transporter were overexpressed in a xylose-
41 assimilating *S. cerevisiae*. Additionally, both the ethanol and glycerol-producing
42 pathways were blocked to enhance malic acid production. The resulting strain produced
43 malic acid from both glucose and xylose, but it produced much higher titers of malic acid
44 from xylose than glucose. When a lower concentration (10 g/L) of xylose was used, the
45 engineered strain produced malic acid with higher yields without ethanol production
46 than when higher xylose concentrations (20 g/L and 40 g/L) were used. As such, a fed-
47 batch culture maintaining xylose concentrations at low levels was conducted and 61.2
48 g/L of malic acid was produced with a productivity of 0.32 g/L·h. Taken together, we
49 successfully engineered *S. cerevisiae* for the production of malic acid from xylose,
50 confirming that xylose offers the efficient production of various biofuels and chemicals
51 by engineered *S. cerevisiae*.

52

53 **1 Introduction**

54 Petroleum-based chemical production is efficient and mature but extensive use of
55 petrochemicals and fossil fuels might lead to environmental problems [1]. With
56 increasing environmental concerns and decreasing oil deposits, there are growing
57 interests in developing technologies to utilize renewable sources for producing fuels and
58 chemicals. Microbial conversion of lignocellulosic biomass into biofuels and chemicals
59 can be a substitute for petroleum-based industries [2]. While corn-starch, sugarcane,
60 and soybeans as the first-generation biomass have been used for the production of
61 biofuels and chemicals, there are ethical issues in utilizing potential food resources for
62 microbial fermentation [3]. In contrast, lignocellulosic biomass can be an ideal substrate
63 for producing biofuels and chemicals as it is not edible and abundant. Lignocellulosic
64 biomass is composed of cellulose, hemicellulose, and lignin. Hydrolysates of cellulose
65 and hemicellulose contain ~70% glucose and 30% xylose [4]. Thus, it is necessary to
66 develop a fermenting microorganism capable of utilizing xylose for the development of
67 economical bioconversion processes using lignocellulosic biomass.

68 *Saccharomyces cerevisiae* is one of the most promising microbial strains for
69 bioconversion of lignocellulosic biomass. While wild-type *S. cerevisiae* cannot use
70 xylose, there have been numerous metabolic engineering efforts to enable *S. cerevisiae*
71 to utilize xylose [5-7]. Two heterologous pathways for xylose metabolism have been
72 introduced into *S. cerevisiae*: the xylose isomerase (XI) pathway and the oxidoreductive
73 pathway consisting of xylose reductase (XR) and xylitol dehydrogenase (XDH) [5]. In
74 both pathways, xylose is isomerized to xylulose and xylulose is subsequently
75 phosphorylated to xylulose-5-phosphate which is further metabolized via the pentose

76 phosphate pathway (PPP) and glycolysis. Additionally, xylose utilization of *S. cerevisiae*
77 has been improved via adaptive laboratory evolution (ALE) under xylose conditions.
78 Currently, it is possible to produce many chemicals and fuels by engineered *S.*
79 *cerevisiae* using xylose [6, 8].

80 *S. cerevisiae* is a Crabtree-positive yeast that produces ethanol exclusively during
81 glucose fermentation regardless of aeration. On the contrary, xylose fermentation by
82 engineered *S. cerevisiae* is not affected by the Crabtree effect, resulting in less ethanol
83 production. Instead, carbon flux from xylose can be redirected to target bioproducts [9,
84 10]. Moreover, because *S. cerevisiae* is generally recognized as safe (GRAS) and a
85 robust microorganism, it is suitable for large-scale industrial fermentation [11].

86 Availability of advanced genetic engineering tools is another advantage of *S. cerevisiae*
87 [12].

88 L-malic acid is a C4-dicarboxylic acid which has been widely used in various
89 industries. Malic acid is commonly used as a food acidulant and beverage ingredient in
90 the food industry. It is also used as a component of cleansers, surfactants, and
91 lubricants in the chemical industry, and an antibacterial agent and physiologically active
92 substances in the pharmaceutical industry [13]. Currently, malic acid is mainly produced
93 by chemical synthesis processes. However, as the chemical processes could generate
94 toxic, non-degradable/recyclable by-products, there are increasing concerns about the
95 safety and sustainability of the chemical processes [14]. Furthermore, only L- malate
96 can be used for food and pharmaceutical products but the chemical synthesis
97 processes generate a mixture of D- and L- malate which is not applicable for the food
98 and pharmaceutical products. On the contrary, as microorganisms produce not D-malic

99 acid but L-malic acid, fermentation-based production processes are more attractive [15,
100 16].

101 Malic acid is an intermediate metabolite of the tricarboxylic acid (TCA) cycle in
102 mitochondria of *S. cerevisiae*. Although there have been efforts to make malic acid via
103 manipulation of mitochondrial TCA cycle genes, malic acid production with a high titer
104 (>60 g/L) and productivity (>0.3 g/L·h) has not been achieved [17-19]. As the TCA cycle
105 is essential for the production of amino acids and energy generation via electron
106 transport chain, genetic perturbations of the genes in the TCA cycle were not effective
107 for producing malic acid but causing growth defects [20]. Recently, it has been reported
108 that high amounts of C4-dicarboxylic acids were produced by activating the cytosolic
109 reductive TCA (rTCA) pathway [21]. In the cytosolic rTCA pathway, pyruvate
110 carboxylase (*PYC1* and *PYC2*) catalyzes the carboxylation of pyruvate into
111 oxaloacetate with CO₂ fixation and ATP consumption. Then, malate dehydrogenase
112 (*MDH3*) converts oxaloacetate into malate with the oxidation of NADH to NAD⁺. Malate
113 is then converted into fumarate by fumarase (*FUM1*) releasing one mole of H₂O, and
114 fumarate is subsequently converted into succinate by fumarate reductase (*FRD1*)
115 (Figure 1). As genetic perturbations to increase metabolic fluxes towards the cytosolic
116 rTCA pathway do not affect regular TCA cycle in mitochondria, it is possible to produce
117 high levels of C4-dicarboxylic acids without growth defects if the reductive rTCA
118 pathway is activated [22-24].

119 In this study, we report the production of malic acid at high titers and productivities
120 from xylose by engineered *S. cerevisiae* with the reductive rTCA pathway. To
121 demonstrate the potential advantages of xylose utilization for the production of malic

122 acid, we assessed malic acid production under glucose and xylose conditions.
123 Additionally, we observed that the malic acid-producing strain exhibited higher malic
124 acid yields without ethanol production with lowering initial xylose concentrations in batch
125 cultures. Thus, a xylose fed-batch culture was performed by intermittently feeding small
126 amounts of xylose to minimize ethanol production and maximize malic acid production.
127 This study demonstrated that xylose is not only abundant sugar in cellulosic
128 hydrolysates but also offers efficient production of malic acids and other C4-dicarboxylic
129 acids by engineered *S. cerevisiae*.

130

131 **2 Materials and methods**

132 **2.1 Plasmid construction**

133 The primers, plasmids, and synthetic DNAs used for plasmid construction are
134 summarized in Table S1, S2, and S3, Supporting Information, respectively. PCR was
135 conducted using Phusion High-Fidelity DNA Polymerase (New England Biolabs,
136 Ipswich, MA, USA). Guide RNA (gRNA) expression cassette targeting *alsS* was
137 amplified using gRNA-alsS-F and gRNA-alsS-R primers, and gRNA expression cassette
138 targeting ME1 was amplified using gRNA-ME1-F and gRNA-ME1-R primers. *alsS* and
139 *ME1* gRNA cassettes were inserted into 2- μ plasmid pRS42H and pRS42K, and they
140 were named pRS42H-alsS and pRS42K-ME1, respectively. To express
141 *Schizosaccharomyces pombe* malate transporter (*SpMAE1*), a codon-optimized
142 *SpMAE1* was synthesized using the gBcoks service from Integrated DNA Technologies
143 (IDT, IA, USA). The protein coding sequence of *SpMAE1* was amplified using
144 dSpMAE1-F and dSpMAE1-R primers, and pRS425GPD vector was amplified using

145 42XGPD-F and 42XGPD-R primers [25]. The two PCR products were combined by
146 Gibson assembly technique [26] and the resulting plasmid was named pRS425GPD-
147 SpMAE1.

148

149 **2.2 Yeast strain construction**

150 This study used the *S. cerevisiae* CBMMP1P2 strain which is a xylose consuming and
151 2,3-butanediol producing strain [27] to construct engineered *S. cerevisiae* strains
152 capable of malic acid from xylose. Plasmids and donor DNAs (dDNAs) were
153 transformed by the lithium acetate/single-stranded carrier DNA/polyethylene glycol
154 method with a CRSPR/Cas9 system [28, 29]. The Cas9-NAT plasmid (Addgene#64329)
155 was transformed into the CBMMP1P2 strain for CRSPR/Cas9 based genetic
156 perturbations. To replace *alsS* located in Chromosome VII (CS6) with the dCS6 DNA,
157 the dCS6 DNA was amplified by dCS6-F and dCS-6R primers and introduced in CS6
158 locus using the pRS42H-alsS plasmid. The resulting strain was named as CTA (Table
159 S4, Supporting Information). The dPDC1-empty DNA containing the homologous
160 regions of the upstream and downstream of the *PDC1* was amplified using dPDC1-del-
161 F and dPDC1-del-R primers and integrated into the *PDC1* locus instead of *ME1* using
162 pRS42K-ME1 plasmid. We named the resulting strain as CTMA (Table S4, Supporting
163 Information). We also integrated the codon optimized *SpMAE1* amplified by dSpMAE1-
164 F and dSpMAE1-R primers into the *PDC1* locus using pRS42K-ME1 and named
165 CTMAE (Table S4, Supporting Information). Thus, *SpMAE1* was under the control of
166 the endogenous *PDC1* promoter and terminator. Each transformant was selected on YP
167 medium (10 g/L yeast extract and 20 g/L peptone) plate containing glucose

168 supplemented with 120 µg/ml nourseothricin and 300 µg/ml Hygromycin B, or 300 µg/ml
169 genetic (G148 sulfate) if required for the selection of transformants. In order to make a
170 prototrophic strain of CTMAE, we sequentially introduced linearized pRS403 (*HIS3*),
171 pRS404 (*TRP1*), pRS405 (*LEU2*), and pRS406 (*URA3*) plasmids into the CTMAE strain
172 and named CTMAE-pro. The information of the engineered strains was summarized in
173 Table S4, Supporting Information.

174

175 **2.3 Flask fermentations**

176 To assess the production of malic acid and other C4-dicarboxylic acids by the
177 engineered strains (CTA, CTMA, and CTMAE) on glucose and xylose in batch cultures,
178 the yeast strains were cultured in 25 mL of YP medium (10 g/L yeast extract and 20 g/L
179 peptone) containing 40 g/L of glucose in a 125-mL flask. Cells were inoculated at an
180 initial optical density at 600 nm (OD₆₀₀) of 1. The cultures were conducted at 30 °C and
181 250 rpm.

182 To investigate effects of xylose concentrations on the production of C4-dicarboxylic
183 acids, the CTMAE strain was cultured in 25 mL of YP medium containing 10 g/L, 20 g/L,
184 and 40 g/L of xylose in 125-mL flasks at an initial OD₆₀₀ of 1. The cultures were
185 conducted at 30 °C and 250 rpm.

186 To examine an effect of biotin on C4-dicarboxylic acids, xylose fed-batch cultures of
187 the CTMAE-pro strain were performed in flasks. The CTMAE-pro strain was inoculated
188 into 25 mL of synthetic complete (SC) medium (6.7 g/L yeast nitrogen base and 0.79
189 g/L complete supplement mixture (MP Biomedicals, Solon, OH, USA)) with or without
190 0.6 mg/L of biotin in 125-mL flasks at an initial OD₆₀₀ of 0.8. In addition, 50 g/L of

191 calcium carbonate (CaCO_3) was used as a neutralizing agent. The cultures were
192 performed at 30 °C and 250 rpm. Initial xylose concentration was 10 g/L and additional
193 xylose was added reaching up to 10 g/L \pm 2 when available xylose was almost depleted.
194 Optical density at OD_{600} was measured using 0.2 M HCl.

195

196 **2.4 Bioreactor fermentations**

197 The fed-batch culture was conducted with 1 L of YP medium in a 3-L bioreactor (BioFlo
198 & CelliGen 115 fermentor, New Brunswick Scientific-Eppendorf, Enfield, CT, USA). The
199 CTMAE strain was inoculated at an initial OD_{600} equal to 6.1 in YP medium containing
200 10 g/L of initial xylose concentration. Additional xylose was added to bioreactor up to 10
201 g/L \pm 2 when available xylose was almost depleted. The cultures were maintained at 30
202 °C. pH was automatically controlled at 6 by adding 2 N KOH solution. The cultures were
203 maintained at 30 °C. Air flow rate varied in the range of 1.5 vvm to 2.5 vvm, and the
204 agitation rate varied in the range of 300 rpm to 500 rpm for aerobic cultures.

205 A xylose fed-batch culture was also conducted with a modified nutrient-rich Verduyn
206 (NRV) medium as described previously [30, 31] in a bioreactor to further increase malic
207 acid production. The CTMAE-pro strain was inoculated in 1 L of the NRV medium
208 containing 10 g/L of an initial xylose concentration in a 3-L bioreactor at an initial OD_{600}
209 equal to 3.9. Additional xylose was added to bioreactor up to 10 g/L \pm 2 when available
210 xylose was almost depleted. pH was automatically controlled at 6 by adding 4 N KOH
211 solution. The cultures were maintained at 30 °C. Air flow rate varied in the range of 2
212 vvm to 6 vvm, and the agitation rate varied in the range of 500 rpm to 650 rpm for
213 aerobic cultures.

214

215 **2.5 Quantitative analysis**

216 Cell growth was monitored by measuring OD₆₀₀ using a UV-visible spectrophotometer
217 (BioMate 3S; Thermo Fisher Scientific, Waltham, MA, USA). The dry cell weight (DCW)
218 was then calculated from the measured OD₆₀₀ by multiplying a conversion factor of 0.41
219 (1 OD₆₀₀ = 0.41 g DCW/L) as described previously [32].

220 Extra- and intracellular metabolites were determined and quantified using a high-
221 performance liquid chromatography (HPLC, Agilent 1200 Series; Agilent Technologies,
222 Wilmington) equipped with a refractive index detector and Rezex ROA-Organic Acid H+
223 (8%) column (Phenomenex Inc., Torrance, CA). Metabolites and sugars were analyzed
224 at 50 °C with 0.005M H₂SO₄ as the mobile phase, and the flow rate was set at 0.6
225 ml/min. The culture broth was centrifuged at 15000 rpm for 10 min, and supernatants
226 were obtained for analyses of extracellular metabolites and sugars in the medium. In
227 order to measure intracellular metabolites, cells were washed three times, concentrated,
228 re-suspended in 250 µL of deionized water, and boiled for 10 min at 100 °C. The boiled
229 samples were centrifuged at 15000 rpm for 10 min, and the supernatants were analyzed
230 by HPLC [33].

231

232 **3 Results**

233 **3.1. Construction of engineered *S. cerevisiae* strains capable of producing malic** 234 **acid from xylose**

235 All genetic perturbations to construct L-malic acid producing *S. cerevisiae* strains began
236 with the CBMMP1P2 strain which was engineered to produce 2,3-butanediol from

237 xylose [27]. In the CBMMP1P2 strain, *GPD1* and *GPD2* were deleted to completely
238 block the glycerol production pathway. In addition, the ethanol pathway was partially
239 blocked by deleting *PDC1* and *ADH1* which are major isozymes for ethanol production
240 in *S. cerevisiae* [34, 35]. A synthetic redox balancing pathway based on a pyruvate-
241 oxaloacetate-malate cycle was installed in the CBMMP1P2 strain for enabling
242 interconversion between NADH and NADPH. Specifically, endogenous promoters of
243 *PYC1* and *PYC2* coding for pyruvate carboxylase were replaced with strong *TEF* and
244 *PGK* promoters, respectively. *MDH3ΔSKL* coding for malate dehydrogenase without a
245 peroxisomal targeting sequence was also expressed to convert oxaloacetate into
246 malate. Finally, *Rhodospiridium toruloides* ME1 converting malate to pyruvate was
247 introduced to complete the cytosolic pyruvate-oxaloacetate-malate cycle.

248 In order to repurpose the 2,3-BDO producing *S. cerevisiae* for the production of
249 malic acid, we first deleted *a/sS* to block the 2,3-BDO pathway in the CBMMP1P2 strain
250 and named CTA. Then, we deleted ME1 in the CTA strain to break the cytosolic
251 pyruvate-oxaloacetate-malate cycle and induce malic acid accumulation and the
252 resulting strain was named CTMA. Therefore, the CTMA strain had the cytosolic rTCA
253 pathway with an increased flux from pyruvate (Figure 1). We also introduced a codon-
254 optimized *SpMAE1* (Table S3, Supporting Information) which is a malate transporter to
255 secrete malic acid into the culture medium, and named the resulting strain as CTMAE
256 (Figure 1) [24]. We then examined the production of malic acid and other C4-
257 dicarboxylic acids by the three engineered strains (CTA, CTMA, and CTMAE) (Table
258 S4, Supporting Information).

259

260 **3.2. Comparison of the production of malic acid from glucose and xylose by**
261 **engineered *S. cerevisiae***

262 We examined the fermentation profiles of the three engineered strains (CTA, CTMA,
263 and CTMAE) under glucose and xylose conditions. First, we compared intracellular
264 concentrations of C4-dicarboxylic acids in the CTA, CMTA, and CTMAE strains in YP
265 medium containing either 40 g/L glucose or 40 g/L xylose under aerobic batch
266 conditions (Figure 2). Malic acid and succinic acid were produced in the three
267 engineered strains (Figures 2A and 2B). As the CTA strain has the pyruvate-
268 oxaloacetate-malate cycle, intracellular malic acid could be detected. As expected, the
269 CTMA strain with the deletion of ME1 converting malic acid to pyruvate accumulated
270 more malic acid than the CTA strain. With introduction of *SpMAE1*, intracellular malic
271 acid concentrations of the CTMAE strain decreased by secreting malic acids into the
272 medium. Similar phenotypes of the CTA, CTMA, CTMAE strains were observed under
273 xylose conditions (Figure 2B). Succinic acid production which is another C4-dicarboxylic
274 acid via the cytosolic rTCA pathway exhibited the same patterns with malic acids under
275 xylose conditions. Under glucose conditions, intracellular malic acid and succinic acid of
276 the CTMAE strain were also remarkably decreased as compared to the CTA and CTMA
277 strains. However, there were no significant differences between the CTA and CTMA
278 strains (Figure 2A). More interestingly, the engineered strains accumulated higher malic
279 acid and succinic acid under xylose conditions than under glucose conditions (Figures
280 2A and 2B).

281 We then investigated extracellular malic acid and succinic acid production. We
282 observed that the CTMAE strain secreted more malic acid and succinic acid than the

283 CTA and CTMA strains under both glucose and xylose conditions (Figure S1 and S2,
284 Supporting Information). Comparing the yields of C4-dicarboxylic acids and ethanol, the
285 CTMAE strain produced more malic acid and succinic acid and less ethanol on xylose
286 than on glucose (Figure 2C). Thus, we focused on xylose conditions for further
287 characterizations to make high levels of C4-dicarboxylic acids from the CTMAE strain.

288

289 **3.3. Effects of xylose concentrations on malic acid production**

290 To investigate effects of xylose concentrations on malic acid production, we conducted
291 aerobic batch cultures of the CTMAE strain in YP medium with 10 g/L, 20 g/L, and 40
292 g/L of xylose (Figure 3; Figure S3, Supporting Information). Ethanol production
293 decreased drastically with reduced initial xylose concentrations. Particularly, the
294 CTMAE strain did not produce ethanol at all under the 10 g/L of xylose conditions.
295 Instead, the CTMAE strain produced more malic acid and succinic acid. As a result,
296 malic acid and succinic acid yields were 70 mg/g xylose and 121 mg/g xylose under the
297 10 g/L of xylose conditions, respectively, which were 2-fold and 2.6-fold higher than
298 those under the 40 g/L xylose conditions. Thus, we expected that malic acid can be
299 produced without ethanol production by maintaining xylose concentrations below 10 g/L
300 via a xylose fed-batch culture.

301

302 **3.4 Effects of biotin on malic acid production**

303 We examined the effects of biotin which is a cofactor of pyruvate carboxylase (PYC) on
304 malic acid production [36]. We hypothesized that biotin might be limiting for PYC activity
305 so that supplementation of biotin might enhance the production of malic acid. We

306 conducted xylose fed-batch cultures of the CTMAE-pro strain in SC medium with or
307 without 0.6 mg/L of biotin in flasks (Figure 4). Xylose was intermittently added to
308 maintain the concentration below 10 g/L. First, we observed that there was no ethanol
309 production during low-level xylose fed-batch cultures as expected. More interestingly,
310 the CTMAE-pro strain showed a malic acid titer of 4.6 g/L and a yield of 0.14 malic acid
311 g/g xylose in SC medium with biotin supplementation, which were 27.6 % and 24.4 %
312 higher as compared to SC medium without biotin supplementation, while the succinic
313 acid titer and yield were not significantly different regardless of biotin supplementation.

314

315 **3.4. Xylose fed-batch culture for malic acid production in a bioreactor**

316 We conducted a xylose-fed batch culture using YP medium under aerobic conditions in
317 a bioreactor (Figure 5A). Once available xylose was almost depleted, additional xylose
318 was added to reach a concentration of 10 ± 2 g/L. The feeding continued until the malic
319 acid titer did not increase further. Through maintaining xylose concentrations at low
320 levels, we were able to increase malic acid production without ethanol production during
321 the fed-batch fermentation, resulting in 18.7 g/L of malic acid for 81.5 h.

322 We then conducted a xylose fed-batch culture using a minimal medium (NRV)
323 containing 0.6 mg/L of biotin in a bioreactor to further increase malic acid production
324 (Figure 5B). As the CTMAE strain is a quadruple auxotroph (LEU-, HIS-, TRP-, and
325 URA-), we constructed a prototrophic strain (CTMAE-pro) after integrating *LEU2*, *HIS3*,
326 *TRP1*, and *URA3* into the CTMAE strain. The CTMAE-pro strain was also cultured
327 under aerobic conditions with intermittent feedings of xylose, maintaining xylose
328 concentrations at low levels (<10 g/L). As a result, cell density reached OD₆₀₀ of 69.2

329 (28.4 g DCW/L) and 61.2 g/L of malic acid was produced. The malic acid yield and
330 productivity were 0.23 g/g xylose and 0.32 g/L·h, respectively. So far, malic acid has
331 been produced from glucose by engineered *S. cerevisiae*. Zelle et al. (2008) produced
332 59.0 g/L of malic acid with a productivity of 0.19 g/L·h of productivity and Chen et al.
333 (2017) reported the production of 30.3 g/L of malic acid with a productivity of 0.32 g/L·h
334 from glucose (Table S5) [24, 37]. Our results exhibited comparable levels of malic acid
335 and productivity from xylose as compared to those reported in a previous study that
336 used glucose for the production of malic acid. Additionally, the CTMAE-pro strain
337 produced 18.5 g/L of succinic acid and 8.0 g/L of fumaric acid. As such, the yield and
338 productivity of total C4 dicarboxylic acids are 0.33 g acids/g xylose and 0.46 g/L·h.

339

340 **4 Discussion**

341 As heavy dependence on petroleum-based industries has led to environmental issues,
342 there is a growing interest in clean and sustainable alternatives such as microbial
343 conversion of renewable biomass into biofuels and chemicals. Among various biomass
344 feedstocks, lignocellulosic biomass is an attractive option because it is not human-
345 edible and abundant substrates. As xylose is one of the major sugars in lignocellulosic
346 biomass, many researchers have made numerous efforts for xylose utilization in *S.*
347 *cerevisiae* which has been widely used in food and pharmaceutical industries [5].
348 Therefore, the production of a variety of biofuels and chemicals from xylose by
349 engineered *S. cerevisiae* has been reported [6].

350 In this study, we demonstrate the efficient production of malic acid and other C4-
351 dicarboxylic acids from xylose by engineered *S. cerevisiae*. In particular, a high-titer

352 production of malic acid from xylose is reported for the first time. We performed
353 metabolic engineering using the CBMMP1P2 strain [27] as a parental strain. As the
354 CBMMP1P2 strain was derived from the *S. cerevisiae* CT2 strain which has the
355 oxidoreductase pathway for xylose utilization [38], the CBMMP1P2 strain was able to
356 consume xylose efficiently. In the CBMMP1P2 strain, the production of glycerol, a major
357 byproduct of *S. cerevisiae*, was completely blocked by deleting *GPD1* and *GPD2*.
358 Additionally, the metabolic pathway responsible for the production of ethanol was
359 partially blocked through deleting *PDC1* and *ADH1*. Complete deletion of *PDC1*, *PDC5*,
360 *PDC6*, *ADH1*, and *ADH2* of the ethanol pathway could lead to severe growth defects
361 because of the limited synthesis of acetyl-CoA, an important precursor of cell growth, in
362 a PDC null *S. cerevisiae* [39-41]. Therefore, only *PDC1* and *ADH1* which encode major
363 isozymes of pyruvate dehydrogenase and alcohol dehydrogenase were deleted in the
364 CBMMP1P2 [34, 35]. Lastly, the CBMMP1P2 strain contained a synthetic metabolic
365 cycle to convert NADH into NADPH via a pyruvate-oxaloacetate-malate cycle.

366 Thus, we took advantage of the phenotypes—elimination of glycerol production,
367 reduction of ethanol production without growth defects, and enhanced metabolic fluxes
368 from pyruvate to malic acid—of the CBMMP1P2 strain for the production malic acid
369 from xylose. The CBMMP1P2 strain was repurposed to a malic acid-producing strain
370 from xylose through the following genetic perturbations. First, we constructed an *a/sS*
371 deletion strain (CTA) to block the 2,3-BOD pathway in the CBMMP1P2. Second, we
372 constructed a ME1 deleted strain (CTMA) to produce malic acid by breaking the
373 pyruvate-oxaloacetate-malate cycle. Third, we introduced *SpMAE1*, a malic acid
374 transporter into the CTMA for constructing the CTMAE strain (Figure 1). These three

375 engineered strains produced not only malic acid, but also succinic acid inside the cells
376 (Figures 2A and 2B). In the cytosolic reductive TCA cycle, fumaric acid can be
377 converted into succinic acid by fumarate reductase using NADH. Typically, NADH is
378 converted into NAD⁺ during glycerol and ethanol production in *S. cerevisiae*. However,
379 as the glycerol and ethanol pathways were blocked in the CTMAE strain, surplus NADH
380 might be used for succinic acid production [42, 43].

381 We then examined malic acid production of the CTMAE strain from 40 g/L of glucose
382 and xylose under aerobic conditions. When xylose was used, the CTMAE strain
383 produced more malic acid and less ethanol than when glucose was used (Figure 2C). *S.*
384 *cerevisiae*, a Crabtree positive yeast produces ethanol rapidly under high glucose
385 concentrations by negatively regulating the genes involved in respiratory energy
386 metabolisms such as the TCA cycle and oxidative phosphorylation [44-46]. According to
387 previous reports, the genes involved in the TCA cycle and oxidative phosphorylation in
388 *S. cerevisiae* are not repressed, or up-regulated under xylose conditions as *S.*
389 *cerevisiae* does not sense xylose as a fermentable carbon source [6, 9, 10]. Thus, the
390 CTMAE strain was able to produce more C4-dicarboxylic acids which are the
391 metabolites of the TCA cycle with less ethanol production when xylose is used as a
392 carbon source.

393 Nevertheless, the CTMAE strain produced a lot of ethanol in the batch culture with
394 40 g/L of xylose. This might be attributed to inhibition of the TCA cycle enzymes by
395 higher fluxes or metabolites in the glycolysis, or possible mis-sensing of xylose by
396 glucose sensors such as Snf3 and Rgt2 as glucose when xylose concentrations are
397 high. To reduce ethanol production from xylose, we examined the effects of initial xylose

398 concentrations (10, 20, and 40 g/L) on ethanol and malic acid production in aerobic
399 batch cultures (Figure 3). As expected, ethanol production decreased and malic acid
400 production increased as the concentrations of xylose reduced. Notably, ethanol
401 production was completely inhibited, and malic acid and succinic acid yields increased
402 drastically under the low xylose condition (10 g/L). We also examined if similar effects
403 can be observed when glucose concentrations are reduced. While ethanol production
404 decreased with reduced glucose concentrations, ethanol was still produced under low
405 glucose (10 g/L of glucose) conditions (Figure S4, Supporting Information).

406 We reason that enhanced production of malic acid and reduction of ethanol
407 production from xylose might be associated with the sugar sensing/signaling
408 mechanism in *S. cerevisiae*. As xylose is structurally similar to glucose, xylose-utilizing
409 *S. cerevisiae* may sense xylose using the glucose-sensing/signaling mechanism such
410 as the Snf3p/Rgt2p pathway [47]. However, xylose-utilizing *S. cerevisiae* exhibited
411 similar gene expression patterns observed in *S. cerevisiae* under low glucose
412 conditions. Thus, cellular physiology under xylose conditions might be similar to that
413 under low glucose conditions where ethanol production is minimized [44, 46].

414 We hypothesized that high levels of malic acid can be produced by the CTMAE
415 strain by maintaining xylose concentrations below 10 g/L in a xylose fed-batch bioreactor.
416 To validate the hypothesis, we first conducted a xylose-fed batch culture in YP medium
417 under aerobic conditions (Figure 5A), and observed that malic acid production
418 increased up to 18.7 g/L without ethanol production. Interestingly, while more succinic
419 acid was produced than malic acid in flask batch cultures, more malic acid was
420 produced than succinic acid in a fed-culture using a bioreactor. We speculate that the

421 shift from succinic acid to malic acid in a bioreactor might be caused by higher
422 aerations. During the fed-batch culture using a bioreactor, we increased both airflow
423 rates and agitation rates to maintain aerobic conditions. Under fully aerobic conditions,
424 surplus NADH can be converted into NAD⁺ using molecular oxygen as an electron
425 acceptor, and fumarate coupled succinic acid production can be minimized. Therefore,
426 malic acid production might be favored over succinic acid production under fully aerobic
427 conditions.

428 Pyruvate is a key metabolite for both ethanol and malic acid producing pathways
429 (Figure 1). We attempted to enhance metabolic fluxes from pyruvate toward
430 oxaloacetate through supplementing biotin which is a cofactor of pyruvate carboxylase
431 [36] and observed that malic acid production can be enhanced when a biotin
432 supplemented medium is used (Figure 4). Thus, we conducted a xylose fed-batch
433 culture using the NRV medium containing 0.6 mg/L of biotin (Figure 5B). Consequently,
434 we were able to increase the malic acid titer and productivity by 61.2 g/L and 0.32 g/L·h,
435 respectively. Zelle et al. (2008) and Chen et al. (2017) reported the production of malic
436 acid from glucose by engineered *S. cerevisiae*. Because the authors deleted all *PDC*
437 genes (*PDC1*, *PDC5*, and *PDC6*) to eliminate ethanol production, malic acid production
438 was accompanied by growth defects [39]. Thus, the higher malic acid titer resulted in
439 the lower productivity or *vice versa* (Table S5) [24, 37]. Furthermore, glycerol was
440 produced as a byproduct in the studies. In contrast, we maintained cell growth by
441 deleting only *PDC1* and *ADH1* in the ethanol-producing pathway and instead controlled
442 ethanol production by a low-level xylose feeding strategy. Besides, we completely
443 prevented the production of another byproduct, glycerol. Additionally, we further

444 enhanced the flux from pyruvate to malic acid using the NRV medium containing the
445 high concentration of biotin which is a cofactor of pyruvate carboxylase. Therefore,
446 malic acid was produced from xylose with a high titer and productivity without growth
447 defects reported in previous studies of malic acid production from glucose.

448 In conclusion, we successfully constructed an engineered *S. cerevisiae* strain
449 capable of producing malic acid from xylose. The CTMAE strain produced more C4-
450 dicarboxylic acids under xylose conditions than under glucose conditions. Furthermore,
451 we achieved a high titer production of malic acid using a xylose fed-batch fermentation.
452 Our results provide effective strategies for using xylose for the biological production of
453 malic acid and other C4-carboxylic acids.

454

455 **Acknowledgment**

456 This study was funded by the DOE Center for Advanced Bioenergy and Bioproducts
457 Innovation (U.S. Department of Energy, Office of Science, Office of Biological and
458 Environmental Research under Award Number DE - SC0018420). Any opinions,
459 findings, and conclusions or recommendations expressed in this publication are those of
460 the author(s) and do not necessarily reflect the views of the U.S. Department of Energy.

461

462 **Conflict of interest**

463 The authors declare no financial or commercial conflict of interest.

464

465 **Author Contributions**

466 **Nam Kyu Kang:** Conceptualization, Investigation, Formal analysis, Methodology,
467 Writing – original draft. **Jae Won Lee:** Conceptualization, Formal analysis,
468 Methodology, Writing - review & editing. **Donald R. Ort:** Supervision, Funding
469 acquisition. **Yong-Su Jin:** Conceptualization, Writing - review & editing, Supervision,
470 Funding acquisition.

471

472 **5 References**

- 473 [1] M. I. Hoffert, K. Caldeira, G. Benford, D. R. Criswell, C. Green, H. Herzog, A. K. Jain, H. S.
474 Kheshgi, K. S. Lackner, J. S. Lewis, H. D. Lightfoot, W. Manheimer, J. C. Mankins, M. E. Mauel, L.
475 J. Perkins, M. E. Schlesinger, T. Volk, T. M. Wigley, *Science* **2002**, 298, 981.
476 [2] S. Chu, A. Majumdar, *Nature* **2012**, 488, 294.
477 [3] D. Graham-Rowe, *Nature* **2011**, 474, S6.
478 [4] A. Carroll, C. Somerville, *Annu. Rev. Plant Biol.* **2009**, 60, 165.
479 [5] S. R. Kim, Y. C. Park, Y. S. Jin, J. H. Seo, *Biotechnol. Adv.* **2013**, 31, 851.
480 [6] S. Kwak, J. H. Jo, E. J. Yun, Y. S. Jin, J. H. Seo, *Biotechnol. Adv.* **2019**, 37, 271.
481 [7] S. Lane, J. Dong, Y.-S. Jin, *Bioresour. Technol.* **2018**, 260, 380.
482 [8] S. Kwak, Y. S. Jin, *Microb Cell Fact* **2017**, 16, 82.
483 [9] Y. S. Jin, J. M. Laplaza, T. W. Jeffries, *Appl Environ Microbiol* **2004**, 70, 6816.
484 [10] A. Matsushika, T. Goshima, T. Hoshino, *Microb Cell Fact* **2014**, 13, 16.
485 [11] C. Auesukaree, A. Damnernsawad, M. Kruatrachue, P. Pokethitiyook, C. Boonchird, Y.
486 Kaneko, S. Harashima, *J. Appl. Genet.* **2009**, 50, 301.
487 [12] G. Guirimand, N. Kulagina, N. Papon, T. Hasunuma, V. Courdavault, *Trends Biotechnol.*
488 **2020**.
489 [13] I. Goldberg, J. S. Rokem, O. Pines, *J. Chem. Technol. Biotechnol.* **2006**, 81, 1601.
490 [14] S. Y. Lee, H. U. Kim, T. U. Chae, J. S. Cho, J. W. Kim, J. H. Shin, D. I. Kim, Y.-S. Ko, W. D. Jang,
491 Y.-S. Jang, *Nat. Catal.* **2019**, 2, 18.
492 [15] I. Goldberg, J. S. Rokem, O. Pines, *Journal of Chemical Technology & Biotechnology* **2006**,
493 81, 1601.
494 [16] J. Liu, J. Li, H.-d. Shin, L. Liu, G. Du, J. Chen, *Bioresour. Technol.* **2017**, 239, 412.
495 [17] T. Asano, N. Kurose, N. Hiraoka, S. Kawakita, *J. Biosci. Bioeng.* **1999**, 88, 258.
496 [18] Y. Arikawa, M. Kobayashi, R. Kodaira, M. Shimosaka, H. Muratsubaki, K. Enomoto, M.
497 Okazaki, *J. Biosci. Bioeng.* **1999**, 87, 333.
498 [19] T. Magarifuchi, K. Goto, Y. Iimura, M. Tadenuma, G. Tamura, *J. Ferment. Bioeng.* **1995**, 80,
499 355.
500 [20] G. Baccolo, G. Stamerra, D. P. Coppola, I. Orlandi, M. Vai, Chapter One - Mitochondrial
501 Metabolism and Aging in Yeast, in: López-Otín, C., Galluzzi, L. (Eds.), *International Review of*
502 *Cell and Molecular Biology*, Academic Press 2018, pp. 1.

503 [21] T. Zhang, C. Ge, L. Deng, T. Tan, F. Wang, *FEMS Microbiol. Lett.* **2015**, 362.
504 [22] D. Yan, C. Wang, J. Zhou, Y. Liu, M. Yang, J. Xing, *Bioresour. Technol.* **2014**, 156, 232.
505 [23] G. Xu, X. Chen, L. Liu, L. Jiang, *Bioresour Technol* **2013**, 148, 91.
506 [24] R. M. Zelle, E. de Hulster, W. A. van Winden, P. de Waard, C. Dijkema, A. A. Winkler, J. M.
507 Geertman, J. P. van Dijken, J. T. Pronk, A. J. van Maris, *Appl. Environ. Microbiol.* **2008**, 74, 2766.
508 [25] T. W. Christianson, R. S. Sikorski, M. Dante, J. H. Shero, P. Hieter, *Gene* **1992**, 110, 119.
509 [26] D. G. Gibson, L. Young, R. Y. Chuang, J. C. Venter, C. A. Hutchison, 3rd, H. O. Smith, *Nat.*
510 *Methods* **2009**, 6, 343.
511 [27] J. W. Lee *Ph.D. Thesis*, University of Illinois at Urbana-Champaign **2019**.
512 [28] R. D. Gietz, R. H. Schiestl, *Nat. Protoc.* **2007**, 2, 31.
513 [29] G. C. Zhang, Kong, II, H. Kim, J. J. Liu, J. H. Cate, Y. S. Jin, *Appl. Environ. Microbiol.* **2014**, 80,
514 7694.
515 [30] S. Lane, Y. Zhang, E. J. Yun, L. Ziolkowski, G. Zhang, Y. S. Jin, J. L. Avalos, *Biotechnol.*
516 *Biofuels* **2019**, 117, 372.
517 [31] P. van Hoek, E. de Hulster, J. P. van Dijken, J. T. Pronk, *Biotechnol. Bioeng.* **2000**, 68, 517.
518 [32] L. Sun, C. A. Atkinson, Y. G. Lee, Y. S. Jin, *Biotechnol. Bioeng.* **2020**, 117, 3522.
519 [33] S. Yu, J.-J. Liu, E. J. Yun, S. Kwak, K. H. Kim, Y.-S. Jin, *Microb. Cell Fact.* **2018**, 17.
520 [34] T. Kondo, H. Tezuka, J. Ishii, F. Matsuda, C. Ogino, A. Kondo, *J. Biotechnol.* **2012**, 159, 32.
521 [35] O. de Smidt, J. C. du Preez, J. Albertyn, *FEMS Yeast Res.* **2008**, 8, 967.
522 [36] M. St Maurice, L. Reinhardt, K. H. Surinya, P. V. Attwood, J. C. Wallace, W. W. Cleland, I.
523 Rayment, *Science* **2007**, 317, 1076.
524 [37] X. Chen, Y. Wang, X. Dong, G. Hu, L. Liu, *Appl. Microbiol. Biotechnol.* **2017**, 101, 4041.
525 [38] C. S. Tsai, Kong, II, A. Lesmana, G. Million, G. C. Zhang, S. R. Kim, Y. S. Jin, *Biotechnol.*
526 *Bioeng.* **2015**, 112, 2406.
527 [39] M. T. Flikweert, M. Swaaf, J. P. Dijken, J. T. Pronk, *FEMS Microbiol. Lett.* **1999**, 174, 73.
528 [40] Y.-G. Lee, J.-H. Seo, *Biotechnol. Biofuels* **2019**, 12, 204.
529 [41] K. Tokuhira, N. Ishida, E. Nagamori, S. Saitoh, T. Onishi, A. Kondo, H. Takahashi, *Appl.*
530 *Microbiol. Biotechnol.* **2009**, 82, 883.
531 [42] I. Borodina, J. Nielsen, *Biotechnol. J.* **2014**, 9, 609.
532 [43] J. H. Ahn, Y.-S. Jang, S. Y. Lee, *Curr. Opin. Biotechnol.* **2016**, 42, 54.
533 [44] T. Pfeiffer, A. Morley, *Front. Mol. Biosci.* **2014**, 1, 17.
534 [45] M. Papini, I. Nookaew, M. Uhlén, J. Nielsen, *Microb. Cell Fact.* **2012**, 11, 136.
535 [46] R. H. De Deken, *J. Gen. Microbiol.* **1966**, 44, 149.
536 [47] K. O. Osiro, D. P. Brink, C. Borgstrom, L. Wasserstrom, M. Carlquist, M. F. Gorwa-
537 Grauslund, *FEMS Yeast Res.* **2018**, 18.
538
539

540 **Figure legends**

541 **Figure 1.** Engineering the biosynthetic pathway of C4-dicarboxylic acids in a xylose-
542 utilizing *S. cerevisiae*. Solid lines indicate single step metabolic reactions, and broken
543 lines indicate multi-step metabolic reactions. Up-regulated genes are shown in blue, and
544 deleted genes are shown in red. Green color indicates metabolic pathways.

545 Abbreviations: DHAP, dihydroxyacetone phosphate; GAP, glyceraldehyde-3-phosphate;
546 G3P, glycerol-3-phosphate; GPD, glyceraldehyde-3-phosphate dehydrogenase; PDC,
547 pyruvate decarboxylase; ADH, alcohol dehydrogenase; xylulose-5-P, xylulose-5-
548 phosphate.

549

550 **Figure 2.** Production of C4-dicarboxylic acids in the engineered strains of *S. cerevisiae*.

551 Intracellular C4-dicarboxylic acid concentrations were measured from the engineered
552 strains grown in YP medium containing A) 40 g/L of glucose for 11 h and B) 40 g/L of
553 xylose for 18 h. C) Extracellular C4-dicarboxylic acid yields of CTMAE strain were
554 measured after grown in YP medium containing 40 g/L of glucose and 40 g/L xylose for
555 14 h and 26 h, respectively. The engineered strains were cultured aerobically in 125-mL
556 flasks with 25 mL working volume at 30 °C and 250 rpm. The data points represent the
557 average of two biological duplicates and error bars indicate standard deviations.

558

559 **Figure 3.** Effects of xylose concentrations on A) malic acid, B) succinic acid, and C)
560 EtOH yields by the CTMAE strain. The cells were cultured aerobically in 125-mL flasks
561 containing 25 mL YP medium with 10 g/L, 20 g/L, and 40 g/L of xylose at 30 °C and 250

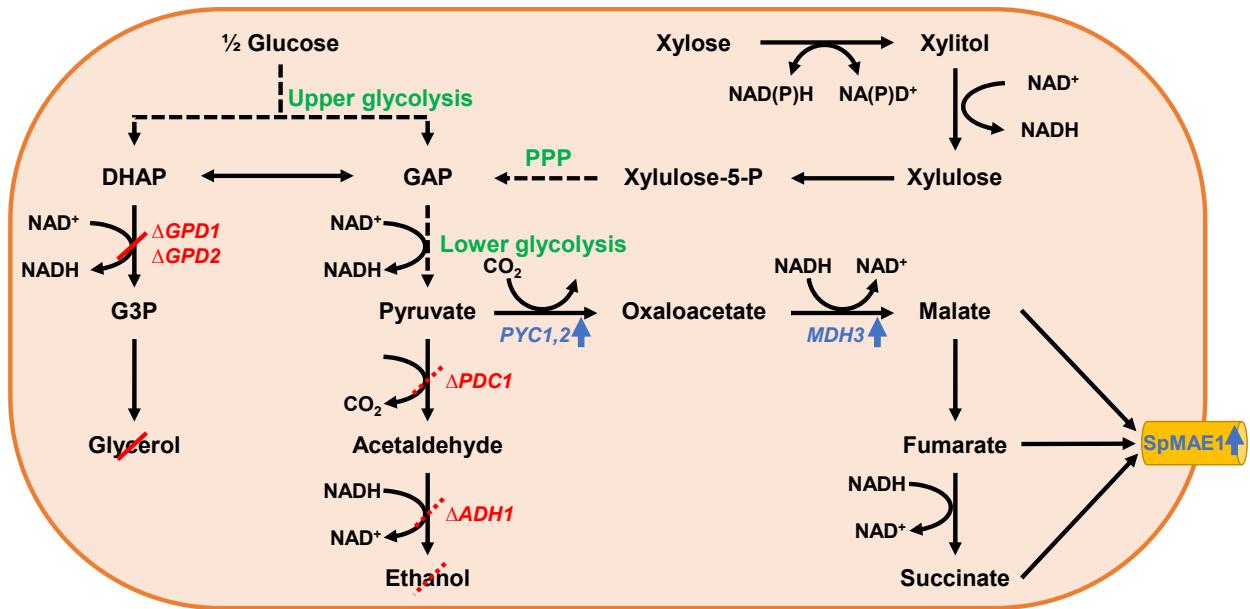
562 rpm. The data points represent the average of two biological duplicates and error bars
563 indicate standard deviations.

564

565 **Figure 4.** Xylose fed-batch cultures of the CTMAE stain in A) SC medium and B) SC
566 medium supplemented with biotin. The cells were cultured aerobically in 125-mL flasks
567 containing 20 mL SC medium with or without supplementation of 0.6 mg/L of biotin. The
568 cultures were maintained at 30 °C. Initial xylose concentration was 10 g/L and additional
569 xylose was added reaching up to near 10 g/L when available xylose was almost
570 depleted. Additionally, 50 g/L of calcium carbonate (CaCO₃) was used as a neutralizing
571 agent. OD₆₀₀ was measured using 0.2 M HCl. The data points represent the average of
572 two biological duplicates and error bars indicate standard deviations.

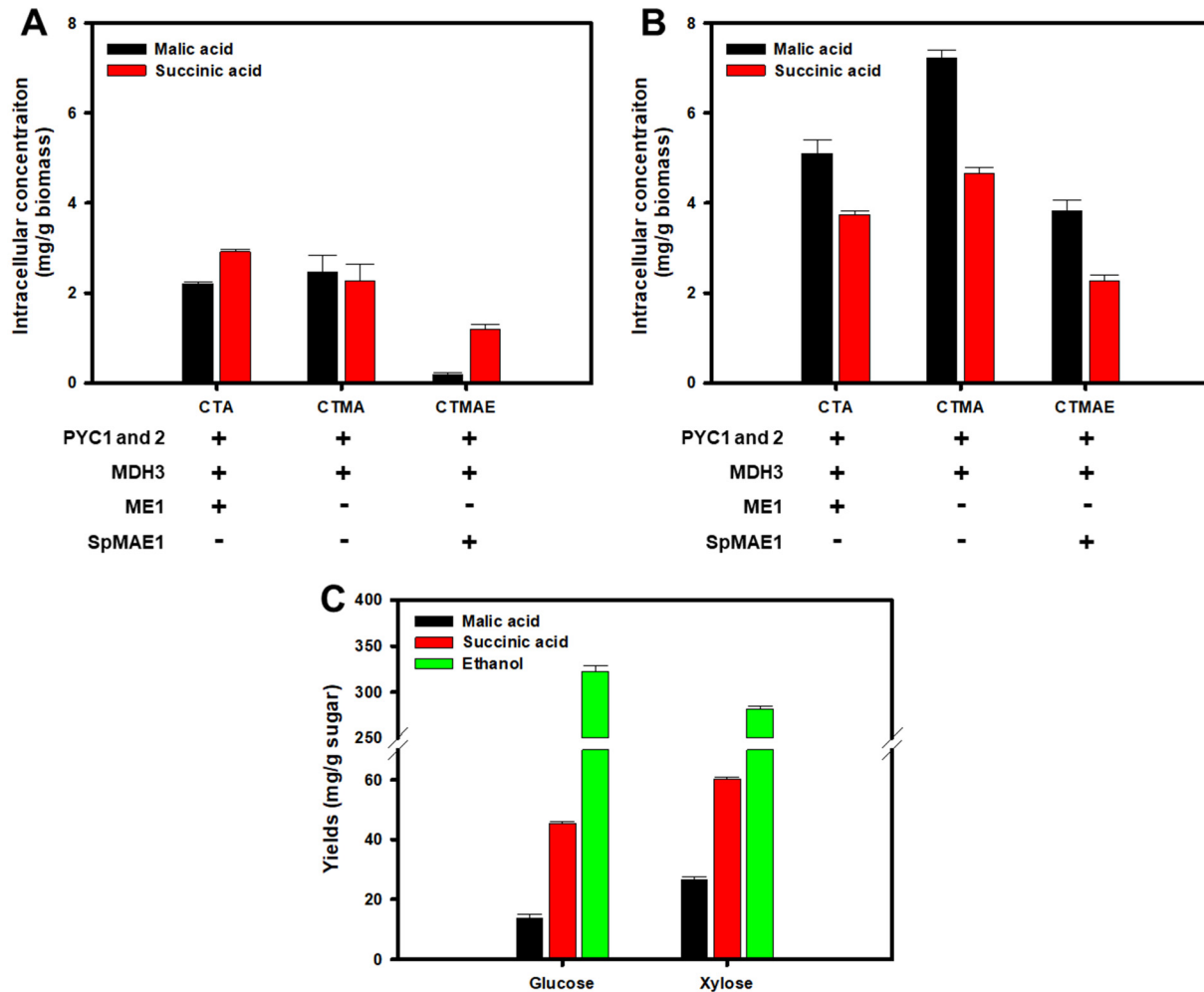
573

574 **Figure 5.** Xylose fed-batch culture of the CTMAE stain in a bioreactor. The cells were
575 cultured aerobically in a 3-L bioreactor with 1 L of A) YP medium and B) the NRV medium.
576 Once available xylose was almost depleted, xylose was intermittently fed to near 10 g/L.
577 pH was maintained at around 6 by 2N KOH for YP medium and 4 N KOH for the NRV
578 medium. The cultures were maintained at 30 °C. The airflow rate varied in the range of
579 1.5 vvm to 2.5 vvm, and the agitation rate varied in the range of 300 rpm to 500 rpm for
580 the xylose fed-batch culture using YP medium. The airflow rate varied in the range of 2
581 vvm to 6 vvm, and the agitation rate varied in the range of 500 rpm to 650 rpm for the
582 xylose fed-batch culture using the NRV medium.



583

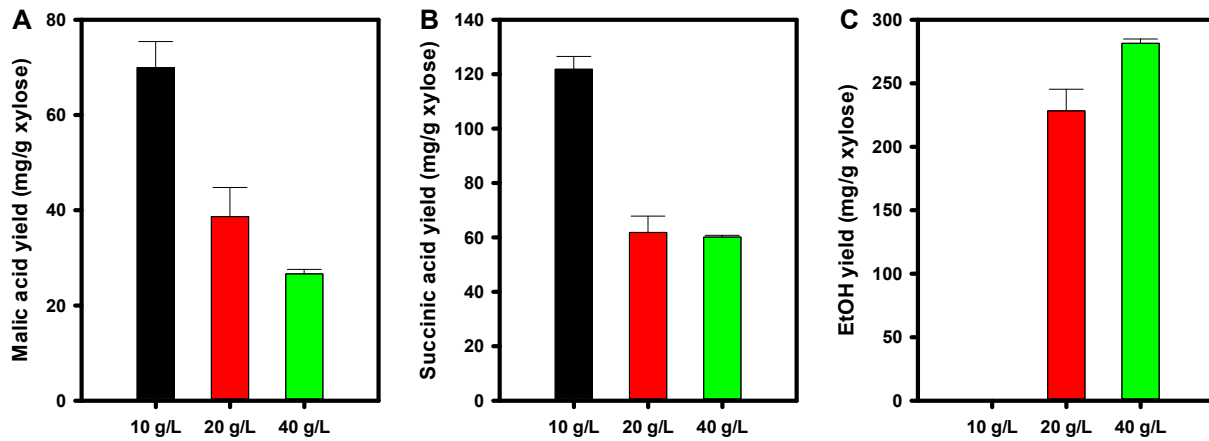
584 **Figure 1.** Engineering the biosynthetic pathway of C4-dicarboxylic acids in a xylose-
 585 utilizing *S. cerevisiae*. Solid lines indicate single step metabolic reactions, and broken
 586 lines indicate multi-step metabolic reactions. Up-regulated genes are shown in blue, and
 587 deleted genes are shown in red. Green color indicates metabolic pathways.
 588 Abbreviations: DHAP, dihydroxyacetone phosphate; GAP, glyceraldehyde-3-phosphate;
 589 G3P, glycerol-3-phosphate; GPD, glyceraldehyde-3-phosphate dehydrogenase; PDC,
 590 pyruvate decarboxylase; ADH, alcohol dehydrogenase; xylulose-5-P, xylulose-5-
 591 phosphate.
 592



594

595 **Figure 2.** Production of C4-dicarboxylic acids in the engineered strains of *S. cerevisiae*.
 596 Intracellular C4-dicarboxylic acid concentrations were measured from the engineered
 597 strains grown in YP medium containing A) 40 g/L of glucose for 11 h and B) 40 g/L of
 598 xylose for 18 h. C) Extracellular C4-dicarboxylic acid yields of CTMAE strain were
 599 measured after grown in YP medium containing 40 g/L of glucose and 40 g/L xylose for
 600 14 h and 26 h, respectively. The engineered strains were cultured aerobically in 125-mL
 601 flasks with 25 mL working volume at 30 °C and 250 rpm. The data points represent the
 602 average of two biological duplicates and error bars indicate standard deviations.
 603

604



605

606

607

608

609

610

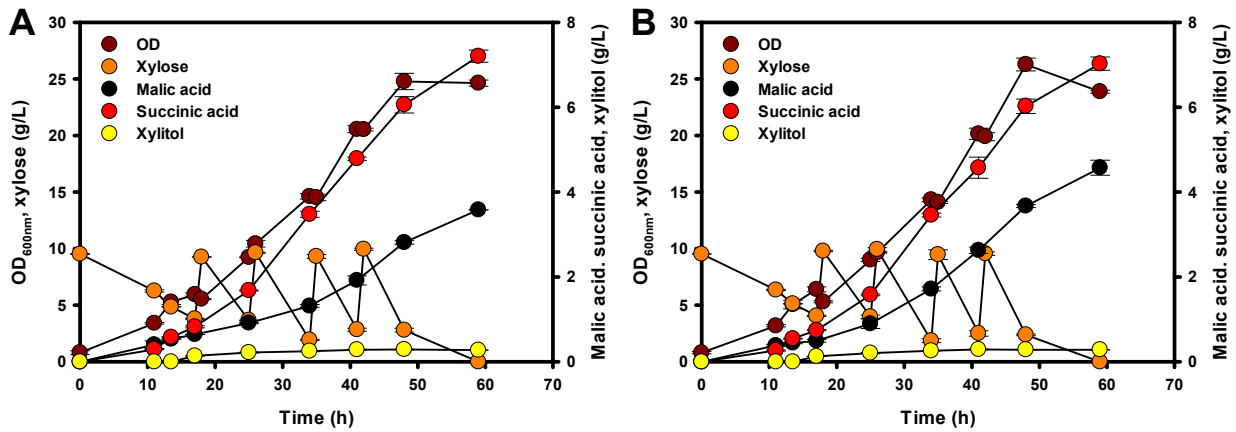
611

612

Figure 3. Effects of xylose concentrations on A) malic acid, B) succinic acid, and C) EtOH yields by the CTMAE strain. The cells were cultured aerobically in 125-mL flasks containing 25 mL YP medium with 10 g/L, 20 g/L, and 40 g/L of xylose at 30 °C and 250 rpm. The data points represent the average of two biological duplicates and error bars indicate standard deviations.

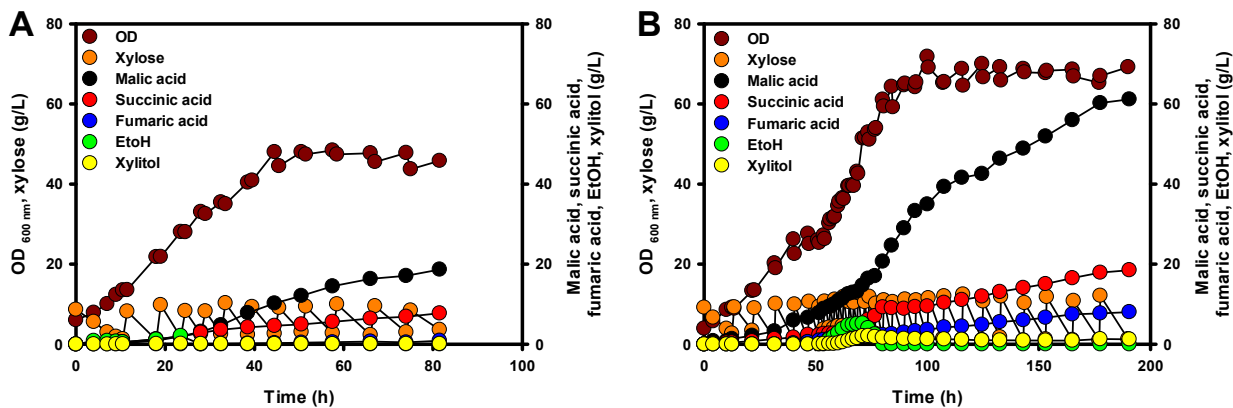
612

613



614

615 **Figure 4.** Xylose fed-batch cultures of the CTMAE stain in A) SC medium and B) SC
616 medium supplemented with biotin. The cells were cultured aerobically in 125-mL flasks
617 containing 20 mL SC medium with or without supplementation of 0.6 mg/L of biotin. The
618 cultures were maintained at 30 °C. Initial xylose concentration was 10 g/L and additional
619 xylose was added reaching up to near 10 g/L when available xylose was almost
620 depleted. Additionally, 50 g/L of calcium carbonate (CaCO₃) was used as a neutralizing
621 agent. OD₆₀₀ was measured using 0.2 M HCl. The data points represent the average of
622 two biological duplicates and error bars indicate standard deviations.
623



624

625 **Figure 5.** Xylose fed-batch culture of the CTMAE stain in a bioreactor. The cells were
 626 cultured aerobically in a 3-L bioreactor with 1 L of A) YP medium and B) the NRV medium.
 627 Once available xylose was almost depleted, xylose was intermittently fed to near 10 g/L.
 628 pH was maintained at around 6 by 2N KOH for YP medium and 4 N KOH for the NRV
 629 medium. The cultures were maintained at 30 °C. The airflow rate varied in the range of
 630 1.5 vvm to 2.5 vvm, and the agitation rate varied in the range of 300 rpm to 500 rpm for
 631 the xylose fed-batch culture using YP medium. The airflow rate varied in the range of 2
 632 vvm to 6 vvm, and the agitation rate varied in the range of 500 rpm to 650 rpm for the
 633 xylose fed-batch culture using the NRV medium.
 634